Tellus
SERIES A DYNAMIC METEOROLOGY AND OCEANOGRAPHY
PUBLISHED BY THE INTERNATIONAL METEOROLOGICAL INSTITUTE IN STOCKHOLM

Tellus (2010), 62A, 551–568

TELLUS

Variable source regions of Denmark Strait and Faroe Bank Channel overflow waters

By ARMIN KÖHL*, *Institut für Meereskunde, Zentrum für Meeres- und Klimaforschung, Universität Hamburg, 20146 Hamburg, Germany*

(Manuscript received 5 August 2009; in final form 23 March 2010)

ABSTRACT

The pathways of the water that overflows the Greenland–Scotland Ridge and their source regions are studied with an ocean circulation model. Depending on the size of wind stress curl around Iceland, different water mass properties are found in the less dense fraction of the overflows on both sides of Iceland. Although in both cases, this fraction contributes to only a small part of the overflow, their pathways and associated source regions characterize also changes in the pathways of the denser fractions which is confirmed by backward float experiments. In detail, large Denmark Strait overflow during high wind stress curl conditions is associated with a primary pathway along the East Greenland Current with one branch encircling the Greenland Sea that is supplied by regions further southward while the other branch enters through Fram Strait. During low forcing conditions, the source region shifts into the Iceland Sea associated with a reversal of a current north of Iceland. The Faroe Bank Channel overflow is primarily fed by sources in the Norwegian Sea with water flowing southward along the Norwegian shelf. A smaller contribution that is enhanced during high forcing follows along the Jan Mayen Ridge and provides water from the Iceland Sea and the Greenland Sea.

1. Introduction

The Nordic Seas are characterized by large water mass transformation due to air–sea interaction and the large property contrast of the inflowing water masses: from the south, warm and saline Atlantic Water that crosses the Greenland-Iceland-Scotland Ridge follows north-eastward within the Norwegian Atlantic Current and enters the Arctic Ocean. As the water is modified along its path, the southward inflow from the Arctic Ocean through Fram Strait is cold and fresh, and flows along the east coast of Greenland; cyclonic circulations within the subbasins characterize the interior flow.

The prominent location of the Nordic Seas between the North Atlantic and the Arctic Ocean causes this area to be one of the most important controlling regions for changes in the Arctic Ocean and North Atlantic while it appears to be also largely affected by circulation changes in these adjacent seas. The water exported via the two main overflow branches through the Denmark Strait (DS) and the Faroe-Shetland Channel (FSC) forms the lower branch of the North Atlantic Deep Water and influences the circulation and water mass properties in the North Atlantic (Schmitz and McCartney, 1993; Dickson and Brown, 1994). An additional smaller part flows over the Iceland-Faroe Ridge. See Fig. 1 for a location of the topographic features in the Nordic Seas. Reduced convection in the Greenland Sea, a decreasing overflow through FSC (Hansen et al., 2001), and the freshening throughout the overflows (Dickson et al., 2002) have been related to the recently described slowing of the Atlantic meridional overturning circulation (Bryden et al., 2005). In this context, Quadfasel and Käse (2007) reported no noticeable trends of the overflow transports during the last decade while variability of the composition has been observed. Along this line, Tanhua et al. (2005) suggest that the overflow might be a robust feature with the ability to switch between different sources.

Model simulations indicate the DS and Faroe Bank Channel (FBC) overflow variability to be in antiphase (Köhl et al., 2007b; Serra et al., 2010). Over the period 1992–2003, the high resolution model simulation of Köhl et al. (2007b) shows in agreement with Biastoch et al. (2003) larger transports through DS from 1997 to 2000 during high wind stress curl forcing and larger transports through FBC after 2001 during low forcing. Changes of the DS overflow were attributed by Köhl et al. (2007b) to changes of the wind stress curl around Iceland and reservoir height changes upstream of the sill. The latter were suggested to be due to circulation changes north of the Greenland Iceland Scotland Ridge which was investigated in further detail by Käse et al. (2009) with a series of idealized experiments. Variable Fram Strait export, local convection or basin wind stress changes were described to lead to changes in the pathways of

*Corresponding author.
e-mail: armin.koehl@zmaw.de
DOI: 10.1111/j.1600-0870.2010.00454.x

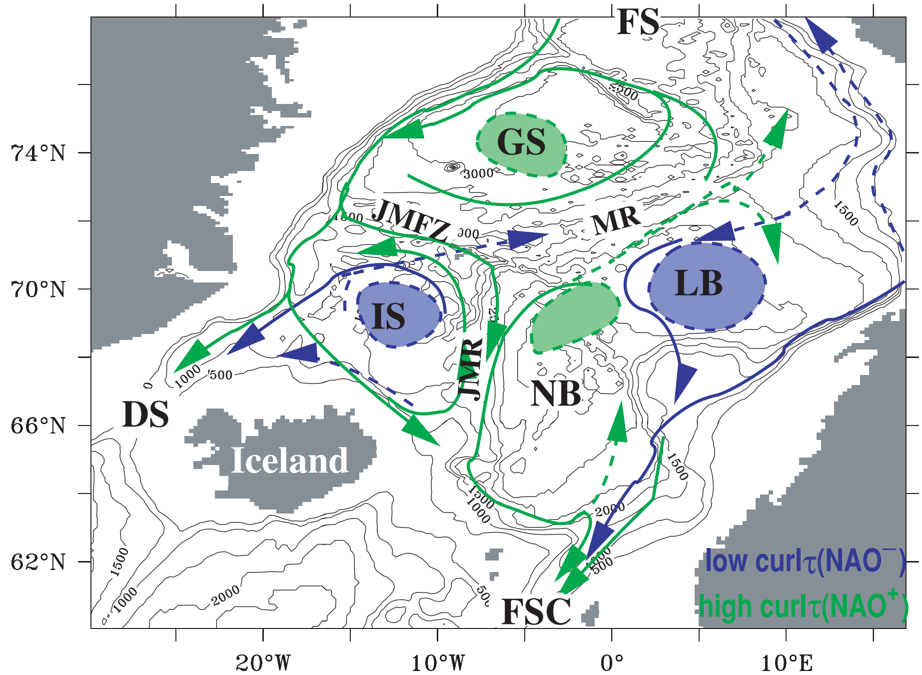

Fig. 1. Schematic of the Nordic Seas with the circulation of water emphasizing different contributing to the overflows during high and low wind stress curl around Iceland that is related to high and low NAO, respectively. The coloured shaded areas indicate larger pools of water that potentially contributes to the overflows. The four major basins are the Lofoten Basin (LB) and the Norwegian Basin (NB) in the east and the Greenland Sea and the Iceland Sea (IS) in the west separated by the Mohn Ridge (MR) which continues to the south as Jan Mayen Ridge (JMR). Dashed lines indicate pathways of overflow water mass types that contribute only indirectly (e.g. through enhancing reservoirs) to the overflows.

dense water in the Nordic Seas. Serra et al. (2010) demonstrate that a large fraction of the wind stress curl variability in the Nordic Seas is related to the NAO and that a relation of the NAO to the DS overflow follows from this. This relation is less clear during certain periods particularly after the mid 1990s. Although measurement-based Denmark Strait overflow estimates by Macrander et al. (2005) and Dickson et al. (2008) suggest a slightly later maximum during the period 1999–2000, the observed FBC transport variability reported by Olsen et al. (2008) is in good agreement with the simulated variability by Köhl et al. (2007b), confirming large FBC transports after 2001.

In the following, we will follow along this line but investigate in greater detail where the source regions of the overflows are, how water overflowing the Greenland Iceland Scotland Ridge propagates towards the sill, and how the source regions and pathways change with forcing changing from high to low wind forcing conditions. As explained in detail later, the study is based to a large extent on the simulation over the period 1992–2004 described by Köhl et al. (2007b). One should keep in mind that this simulation has some shortcomings concerning a missing spinup, the length of the run and the boundary conditions that are provided by a global synthesis. After a brief presentation of the simulation and methodological aspects, Section 3 describes changing water masses at the DS and the changes of associated upstream pathways of these water masses. Section 4 then explains changing water masses at FSC and the changes of associated upstream pathways. In Section 5, adjoint sensitivities are used to describe the relation between the overflows at DS and FBC and how upstream density signals affect both overflows. We finish with concluding remarks in Section 6.

2. Methodology

As the previous study by Käse et al. (2009), the analysis is based on the model results of Köhl et al. (2007b) who also describe the model setup in greater detail. The numerical model was set up for the region of the Nordic Seas including the western subpolar Atlantic from 51°N to 78°N and from 46°W to 17°E. It is nested into the global 1° global synthesis of Köhl et al. (2007a). The grid is horizontally isotropic with a zonal resolution of 1/10° and has 30 levels in the vertical. Coefficients of biharmonic horizontal diffusion and viscosity vary spatially with the cube of the horizontal grid spacing and have equatorial values of 10^{10} m^4 s^{-1}. After starting from rest and climatological Levitus and Boyer (1994), Levitus et al. (1994) temperature and salinity in 1992, the simulation was forced over the period 1992–2004 by the daily atmospheric state obtained from the NCEP/NCAR reanalysis project using bulk formula according to Large and Yaeger (2004). Vertical mixing is parameterized by the K-profile parametrization (KPP) scheme of Large et al.

(1994) and a dynamic/thermodynamic sea ice model of Zhang and Rothrock (2000) is applied. For adjoint sensitivity studies, a low-resolution twin version of this configuration was set up which has an isotropic horizontal resolution of 1/4° with equatorial values of 4×10^{11} m^4 s^{-1} for horizontal diffusion and viscosity. Both models were based on the MITgcm code that is designed to allow the construction of the adjoint by the automatic differentiation tool TAF (Transformation of Algorithms in Fortran) (Giering and Kaminski, 1998) which was used to generate the adjoint model. As in Hoteit et al. (2005), we use larger viscosities in the adjoint to prevent it from developing unstable modes. To this end, an additional viscosity of 10^4 m^2 s^{-1} was employed in the adjoint model. Backward float trajectories were calculated offline based on linearly interpolated 3-day snapshots of the three-dimensional velocities from the high-resolution model output.

3. Changing water masses and pathways of the Denmark Strait Overflow

Swift and Aagaard (1981) described the main source of the DS overflow as originating from the Iceland Sea and Smethie and Swift (1989) then related the dense part of the overflow to the intermediate water in the Greenland Sea. However, a complementary circulation scheme was presented by Mauritzen (1996) who describes the origin of the overflow water as originating from 3 branches of the Norwegian Atlantic Current that, after transformation in the Arctic Ocean and at Fram Strait, return as East Greenland Current (EGC). The two branches that either flow westward in the Fram Strait or northward through Fram Strait supply the DS overflow water while the flow through the Barents Sea opening form the FBC overflow. It was realized over the years that several different water masses contribute to the overflow and that, on its route along the Greenland slope, the EGC exchanges waters with the Greenland and Iceland Seas and incorporates additional intermediate water masses (Rudels et al., 2002). The common notion nowadays is that Arctic Atlantic Water and upper Polar Deep Water, with contribution from Return Atlantic Water (RAW) and Icelandic Arctic Intermediate Water (IAIW), form the main constituents of the DS overflow. However, this view is still not generally accepted, especially since Jonsson (1999) argues that a westward current north of Iceland suggests the Iceland Sea as the main contributor to the DS overflow.

Rudels et al. (2003) described, for the first time, that the pathways of the water supplying the DS overflow may not be as steady as present-day circulation schemes may suggest. By comparing water masses derived from hydrographic observations taken in the early and late 1990s upstream of DS, they found temporal variations in the composition of source water masses and concluded that this also indicates a possibility for a temporal change in the upstream pathways. As temporal variability in the strength of the overflows was found by Köhl et al. (2007b), which was related to upstream circulation changes due to changing forcing conditions by Köhl et al. (2007b) and Käse et al. (2009), it seems reasonable to try to investigate the associated changes in water mass properties in this model simulation. Although the simulation of water mass properties including their spreading, particularly downstream of the overflows, is according to Willebrand et al. (2001) among the weakest capabilities of present-day ocean models, their work also suggests that water mass properties are adjusting relatively slowly. Although, the above-mentioned shortcomings of the Köhl et al. (2007b) simulation, for example the lack of spinup and the short integration time, promised to be an advantage since the background ocean state remains relatively close to the climatology, a further investigation revealed that water masses, for example in the East Greenland Current, are also not correctly represented in the climatology. The model state is therefore biased from the beginning, a fact that has to be taken into consideration when comparing to observed water mass characteristics.

For different years, Fig. 2 shows TS-diagrams of the water masses in the Denmark taken along a section just upstream of the sill where diapycnal mixing associated with the overflows has not yet impact the water mass properties and across which previous transports by Köhl et al. (2007b) were calculated. The section encompasses only the latitudes where densities larger than $\sigma = 27.8$ exist and excludes thus most of the Polar Surface Water and the Atlantic inflow. The years 1994 and 2003 correspond to low wind stress forcing around Iceland and are characterized by relatively warm and saline conditions while during stronger forcing in 1999 the water is colder and fresher. As mentioned before, these water masses can not be compared without corrections to the T-S characteristics from hydrographic sections, for example the T-S diagram shown in Fig. 6 of Rudels et al. (2002) and Fig. 4 of Rudels et al. (2003). Their sections across the entrance of the DS (roughly along 23°W only 2° eastward of our definition) were taken in 1990 and 1998, years of very high and relatively high NAO, respectively. The modelled water masses in the East Greenland Current are biased to low temperatures reaching hardly a temperature maximum of 1 °C as compared to the observed maximum of around 2 °C. This is owing to the fact that not even the climatology the model was start from provides correct T-S characteristics. As the temperature maximum in the East Greenland Current decreases due to mixing with colder and fresher water along its way towards the DS (see Rudels et al., 2003), their TS-diagram from the 1998 section taken in a year with large wind stress with maximum temperatures around 1.5 °C should be compared with the simulated characteristics of maximum temperatures just below 1 °C in 1999. Consequently, both water masses describe mainly sources from the East Greenland Current.

Rudels et al. (2002) concluded that the even colder and fresher water masses (below 1 °C) seen in their earlier observation, taken during even higher NAO in year 1990 points at a source from the Iceland Sea. This case is not realized during the model run

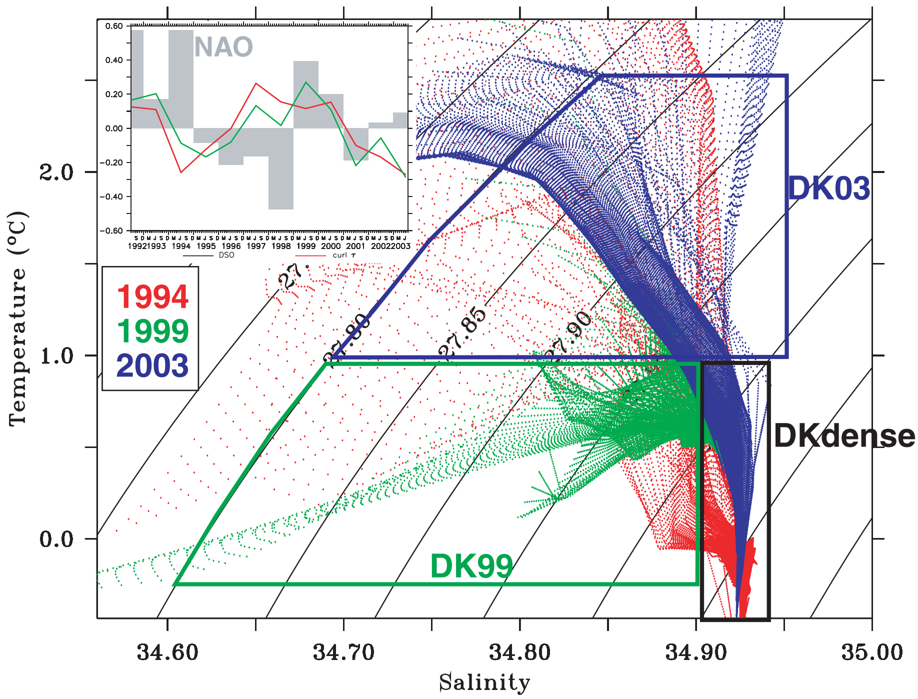

Fig. 2. T-S diagram of the water masses in the Denmark Strait sampled along 26°W between 66.6°N and 68.0°N in three different years as indicated. The definition of the three water mass classes is indicated by boxes in the corresponding colour. The black box defines the densest class with a lower boundary at 1.2 °C not visible on the plot. The TS-characteristics of 1999 is typical for the period 1995–2001, the remaining years correspond to the characteristics of 1994 and 2003. The small inset shows the annual mean NAO Index from NOAA Climate Prediction Center for the period 1992–2003 and the DS overflow together with the wind stress curl averaged over the region around Iceland and scaled as in Fig. 7 of Köhl et al. (2007b).

which instead realizes two cases of low wind stress forcing. Although the tendency of the model seem to be correct that during higher wind stress curl situations (e.g. from 1994 to 1999) the temperatures in the Denmark Strait are lower we will show in the following that the associated circulation changes are quite different from the tendency that is observed for the transition from high (in 1998) to even higher NAO in 1990. Eldevik et al. (2009) presented an analysis of temperature and salinity changes in the Nordic Seas for the period 1950 to 2005. As in the model, they find a general warming and salinification trend in the DS overflow from 1999 to 2003, although 1999 and 2003 do not appear as particular extreme cases in their analysis. Opposing a simple relation to the NAO or wind stress curl, 1990 appears to be relative warm and salty.

According to Rudels et al. (2003), on time scales from month to years, variable wind forcing controls the sources to be either from the Iceland Sea or from the EGC. On longer time scales, the Greenland Sea convection is the key to the variable water masses. Strong convection forces the Recirculating Atlantic Water (RAW) to dominate in the EGC and in the DS overflow whereas low convection causes more Arctic Atlantic Water to enter the EGC. By tracing back the different water masses, we will try to asses, if changing pathways and origins can be revealed. For the lighter fraction of the overflow, roughly water of $\sigma_\Theta < 28.0$, water mass properties for the year 1999 and 2003 almost perfectly separate into two disjunct classes, allowing for a simple definition of two classes, DK99 and DK03, as indicated by the green and blue boundaries in Fig. 2. For the remaining dense part, only one class (DKdense) is defined as indicated by the black box. These simplified definition of water mass classes are chosen to provide a comprehensive classification of many complicated processed associated with formation and mixing of water masses that the model is not expected to represent correctly although it expected that the imprint of larger circulation shifts on the water mass characteristics are represented sufficiently correctly.

Comparing layer thicknesses of the three classes and how they transform from high to low wind stress curl conditions (Fig. 3), reveals a major switch in the circulation regime. From 1999 to 2003, the main pathway of water exiting through the DS changes from an almost exclusive EGC source to a dominant source in the Iceland Sea. At the same time, the pool of DK03 water in the Iceland Sea has shifted towards the northwest while the volume has not changed much (Figs. 3c and d). The origin of the warm and salty water masses needs further explanation. In the model, the warm and salty water that is found in the near surface depths (depth range 40–300 m) of the Iceland Sea shares some characteristics with the Recirculating Atlantic Water, that can be found

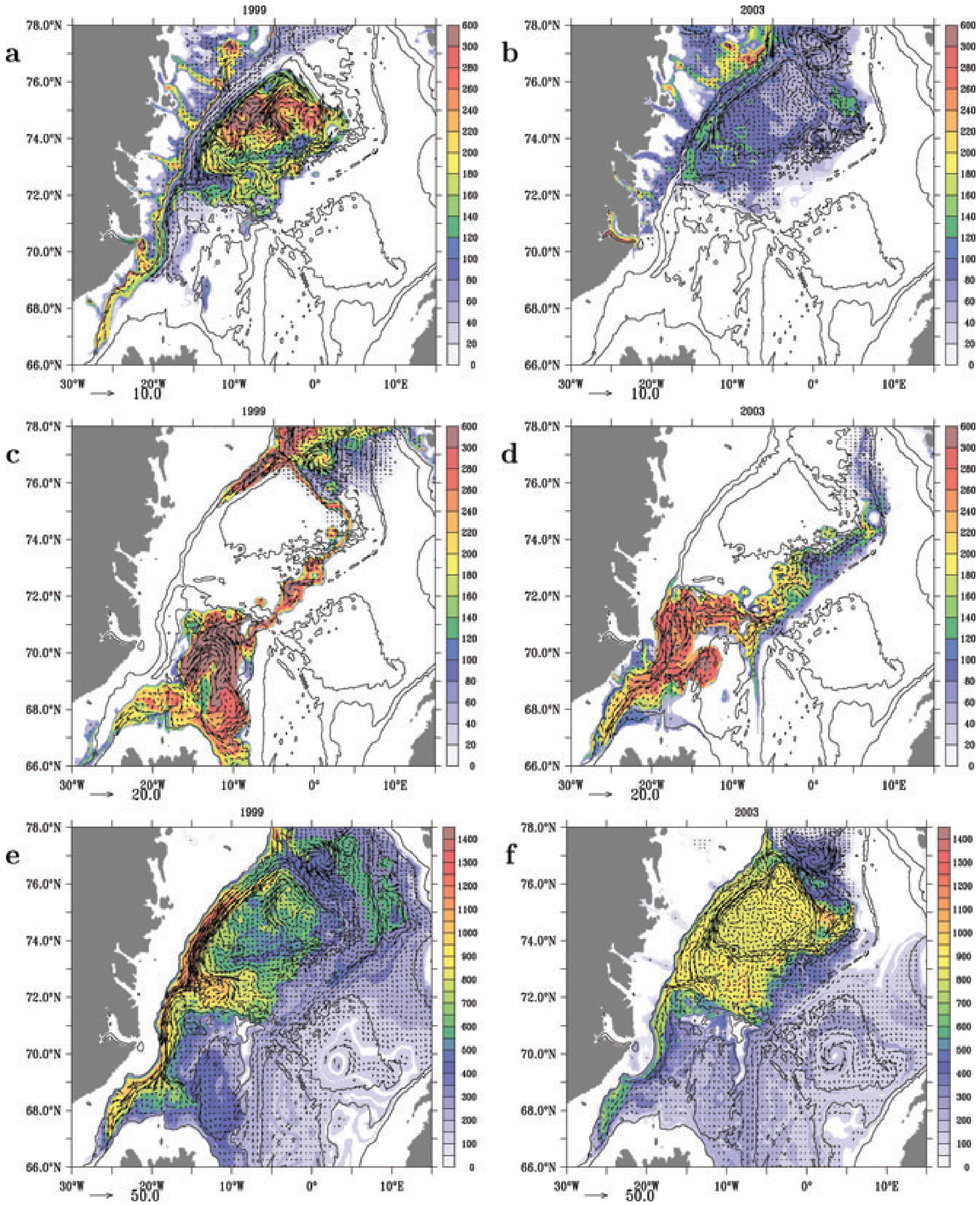

Fig. 3. Layer thickness (in m) of different water mass classes. Shown are years of high and low wind stress curl (1999,2003), respectively for the classes DK99 (a,b), DK03 (c,d) and DKdense (e,f). Volume transports (in m^2 s^{-1}) from vertically integrated velocities in the respective layer are overlaid.

in the Fram Strait, rather than the signal of the Recirculating Atlantic Water near the Denmark Strait. It originates from water of the Irminger Current that is entrained and advected with the westward current north of Iceland. Further on its cyclonic path around the Iceland Sea, it includes water from the Arctic Front which carried with the northward current along the Mohn ridge. It then circulates westward south of the Jan Mayen Fracture Zone penetrating into the Iceland Sea. These water masses mix Atlantic water with the fresher and colder water of the Iceland Sea resulting into characteristics that resemble the Recirculating Atlantic Water. The creation of this water is associated with a stronger cyclonic circulation in the Iceland Sea while this water gets exported during the following period of low wind stress forcing when the cyclonic circulation relaxes. Recent combined observations from Argo profiles reveal in fall 2006 some indication of a northward spreading of warm and salty water along

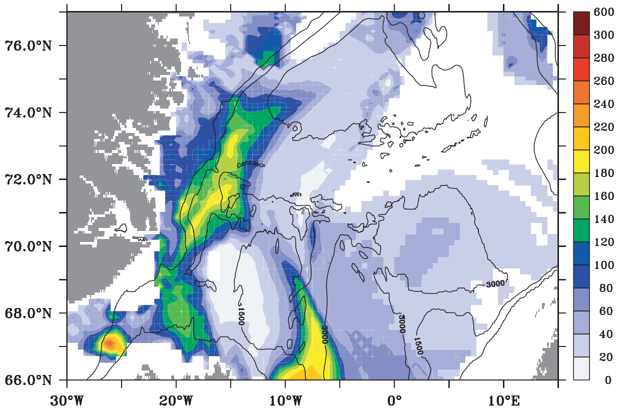

Fig. 4. Layer thickness (in m) of the water mass classes DK03 calculated from the objectively analyzed Argo temperature and salinity profiles provided by Gaillard et al. (2009).

the Jan Mayen Ridge followed by a westward advection into the Iceland Sea south of the Jan Mayen Fracture Zone (Fig. 4). This pathway of near surface water is also indicated by the drifter trajectories show by Poulain et al. (1996) (their Fig. 4 and Scheme 7), although one has to keep in mind that drifters are moving slightly above this layer.

During the period 1999 to 2003, the large pool of cold and fresh water (DK99, in panels a and b) in the Greenland Sea has ceased and been replaced by denser water (DKdense), which was concentrated in the EGC in 1999 and is more spread out towards the east in 2003 (Figs 3e and f). From 1999 to 2003, changes in respective volumes north of the Greenland Iceland Scotland Ridge are summarized in Fig. 5a showing a constant DK03 volume and a reduction of DK99 by 50%. However, the largest changes are visible in the dense fraction with a build up of volume in the period 1995–2000 during low wind stress curl conditions and a decrease thereafter. At interdecadal time scales, a relation of deep convection in the Greenland Sea to negative NAO phases has been discussed previously by Dickson et al. (1996) which was confirmed in the present simulation by Käse et al. (2009). However, the study by Häkkinen (2007), similar to Rudels et al. (2003), emphasizes advection and mixing of Atlantic and Arctic water masses as the most critical aspect in leading to deep water renewal in the Greenland Sea. After the large DS overflow during 1997–1999, the volume of DKdense fraction has increased in the Greenland Sea and the gain in dense water (DKdense) at expense of the lighter fraction (DK99) is provided by upward displacement of the upper boundary of the dense fraction from 350 to 150 m depth (not shown) which points at a local source of dense water through convection. In the Greenland Sea the total thickness of the upper and lower layer together (DK99+DKdense) has not changed significantly indicating that no major net advection out of basin has taken place.

Considering the associated transports shown as overlaid vectors in Fig. 3, the contribution from the EGC has disappeared completely in the lighter fraction and is replaced by a source of DK03 water from the Iceland Sea. In the dense fraction (Figs 3e and f), the Iceland Sea has changed from a net receiver of dense water from the EGC to a net source of dense water for the flow into the DS. Between 68°N and 69°N dense water is entering the Iceland Sea and flowing eastward with the East Icelandic Current in 1999 while in 2003 the currents reverse, leading to contribution from two paths, one southward from the northern part of the Iceland Sea and a westward flow north of Iceland. Note, that the westward current across the Hornbanki section (21.5°W), which Jónsson and Valdimarsson (2004) suggested as an indicator for the main source of the DS overflow being located in the Iceland Sea, is always westward as also the transport time series of Köhl et al. (2007b) demonstrate, although the contributions to this current switch from the EGC in 1999 to sources from the Iceland Sea in 2003. According to the modelling results, the presence of this current is therefore not a sufficient indicator for a source in the Iceland Sea.

Timeseries of a decomposition of the DS overflow into the contributions from the three water masses are shown in Fig. 5b together with the total overflow. Most noticeable is the small contribution from the lighter water masses that contribute with 0.6 Sv to only about 25% of the total overflow. In comparison, observational data from a seven-section mean suggest a larger fraction of the transport in the density range $27.8 < \sigma_\Theta < 27.95$ of about 40% (Plate 1 of Girton et al., 2001). However, the range of values from the observations is rather large and their model results show roughly the same low value as the present simulation. Accordingly, estimates from some individual sections, particularly those further upstream, provide even lower values than the models. Results of the present model show that already downstream of 27°W entrainment starts to play a role which may account for the differences. The contribution from DK99 disappears after 2001 while the contribution from DK03 increases over the period 1999–2003 from 0.2 to 0.6 Sv largely balancing the decrease in DK99. The total DS overflow variability follows thus the variability of the dense fraction which decreases by about 0.4 Sv over the same period. Although the contributions from the lighter fractions are small and seem to balance each other, they carry almost an equal amount of variability as the dense fraction. This is remarkable since the total volume of DK99 and DK03 and its variability is much smaller than those of DKdense. At the same time, the inflow of Atlantic Water stays constant over the period 1999 to 2003 whereas the outflow of Polar Surface Water reduces from 1.14 to 0.24 Sv (not shown).

Regarding only layer transports, the actual pathways of water cannot clearly be identified. Particularly, it remains unclear how much water from the EGC is provided to the DS overflow in comparison to contributions from the Iceland Sea in the years 1999 as opposed to 2003 and whether water from the centre

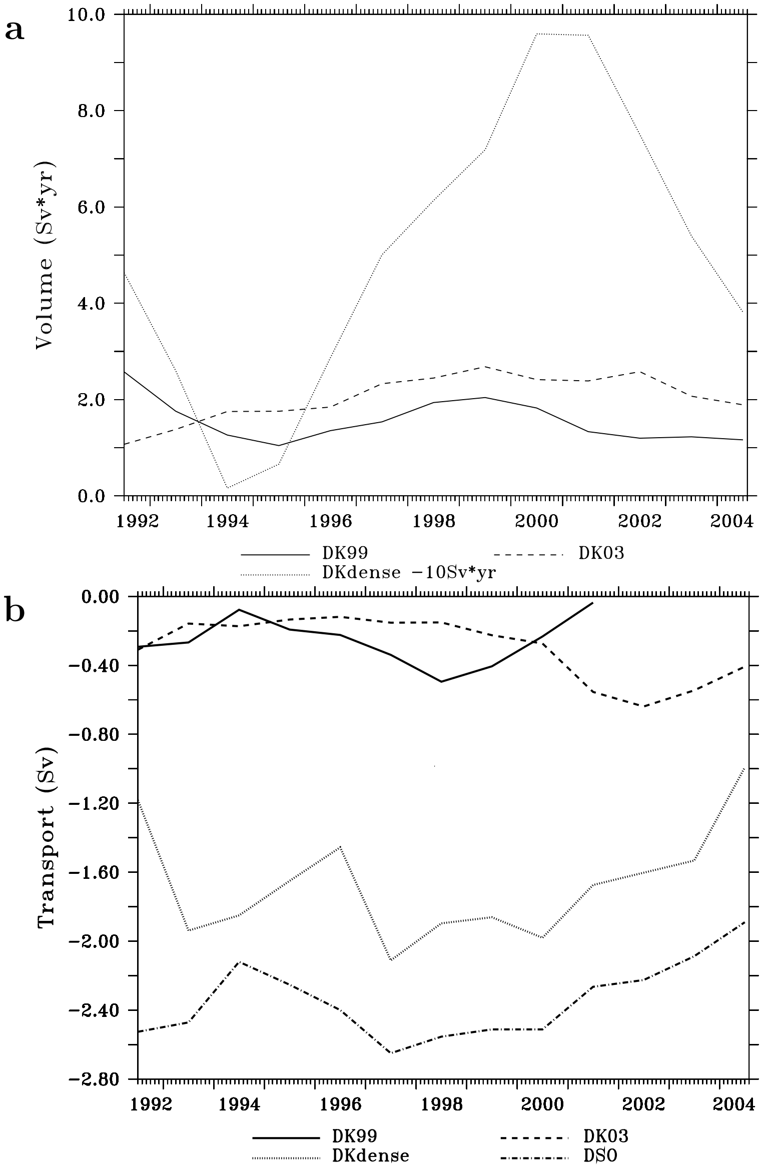

Fig. 5. Total volume of water in the density classes DK99, DK03, and DKdense (a) and their contributions to the DS overflow calculated as transports across 25°W below $\sigma_\Theta = 27.8$ (b).

of Greenland Sea contributes to the DS overflow. To separate the paths that actually contribute to the DS overflow from water of the same type that is just recirculating, floats were seeded upstream of the overflow and followed backward in time. The trajectories reveal the purely advective pathways. Mixing is only taken into account as far as it is represented by resolved eddies. DS overflow transports show a noticeable seasonal cycle with larger transports during early winter. However, separate backward calculations for floats seeded in winter and summer do not reveal any dependence on the season (not shown). Snapshots of float positions after 180, 360 and 720 days of backward integrations in year 1999 and 2003, respectively, shown in Fig. 6 reveal a distinct shift in pathways that basically reflects the changes discussed above for the light fractions (the additional route south of the ridges is due to water from the overflows east of Iceland that is either entrained into the overflow or part of the inflowing water into which some of the floats were inevitably seeded). An additional contribution from the shallow inflow on the shelf through Fram Strait is visible. In year 1999, the main contribution is from the EGC with a small part from the Iceland Sea that appears to be due to eddy mixing.

Over the course of the 4 years of backward integration, about 30% of the floats exiting through the DS came through the Fram Strait. At 360 days ago shown in Fig. 6c only 8% are north of 78°N but about 20% are in the eastern Greenland Sea, at the western flank of the Mohn Ridge. Inspecting the TS characteristics of the floats, the larger part of the latter floats have salinities larger than 34.8 and show a positive slope in the TS diagram

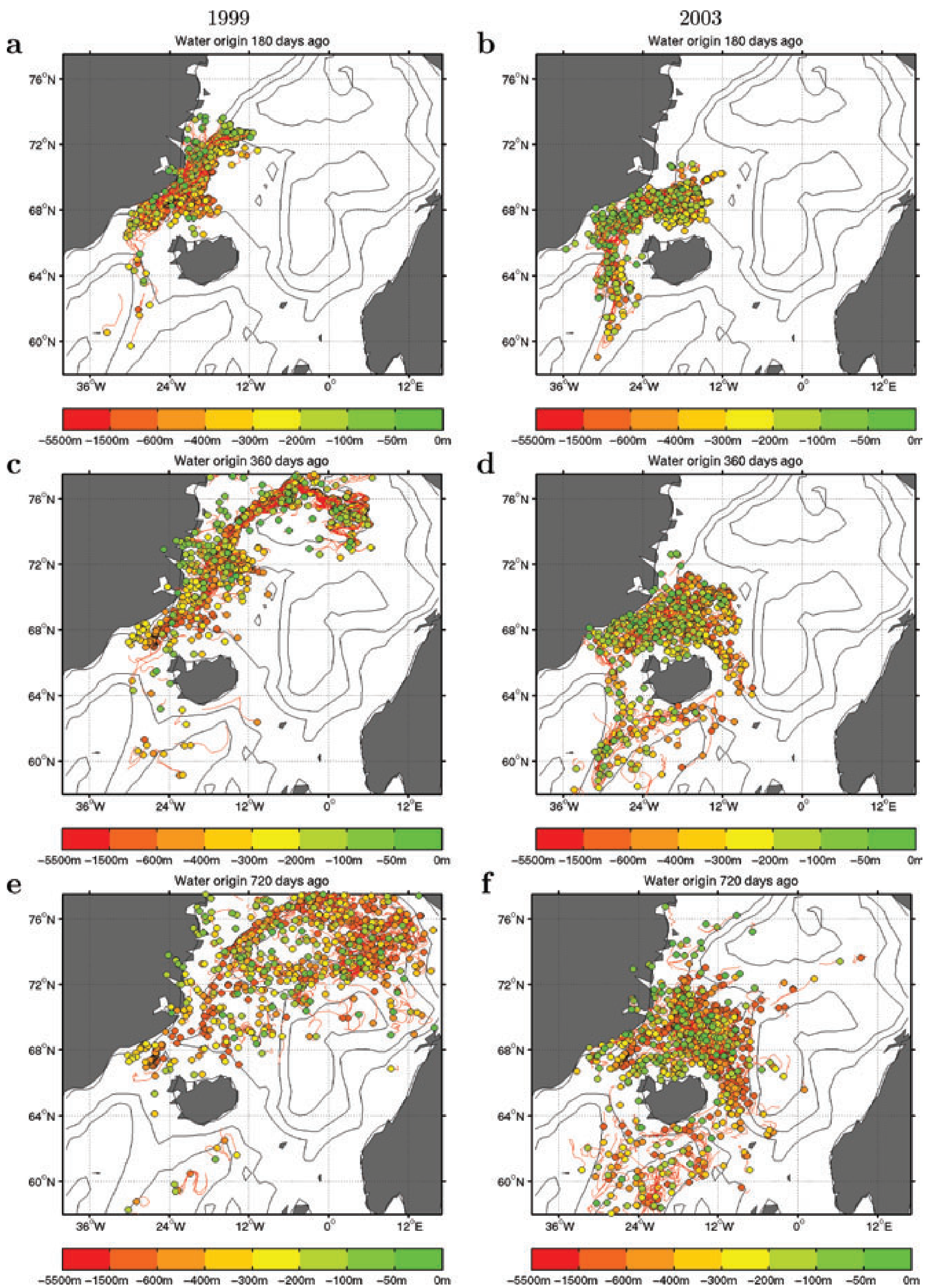

Fig. 6. Backward float positions with a path from the last 30 days and depth indicated by colour. 1000 floats were seeded along 26°W roughly below $\sigma_\Theta = 27.8$ in year 1999 (left panels) and 2003 (right panels), respectively and integrated backward for periods as indicated in the panels. Floats were not strictly seeded in southwestward moving water therefore some of the floats follow the pathways south of the Greenland Iceland Scotland Ridge.

indicating RAW whereas a smaller fraction is colder and fresher (not shown). As we go further back in time (Fig. 6e), the larger fraction is originating from regions southeast while the smaller fraction originates from moving along the Jan Mayen Fracture Zone and then continuing along the Mohn Ridge, these indicate Arctic Ocean water that is branching off the EGC and than is cyclonically moving around the Greenland Sea. Note, that water from the centre of the Greenland Sea hardly contributes to the overflowing water. The traveltime from the Fram Strait to the DS of about 1 year is in agreement with other studies (Olsson et al., 2005; Eldevik et al., 2009). In 2003, the pathway entirely shifts to a source in the Iceland Sea. For longer time scales, smaller contributions from EGC, the Jan Mayen Current, and even the Norwegian Sea become visible. There are no distinctively different pathways visible for deeper (denser) as opposed to the lighter fractions. The purely advective pathways reveal thus a clear separation of the regimes for high and low wind stress curl conditions.

For spring 2002, Jeansson et al. (2008) describes the East Greenland Current to be the main source for the waters found at the Denmark Strait Sill. The East Greenland Current carried water masses from different source regions in the Arctic Ocean, the West Spitsbergen Current and the Greenland Sea. A separate calculation with floats seeded in spring 2001 (not shown) revealed that the simulated path has already switched to the source in the Iceland Sea confirming the earlier notation that the simulated changes are earlier in time.

4. Changing water masses and pathways of the Faroe Bank Overflow

Aagaard et al. (1985) suggest Norwegian Sea Deep Water mixed with intermediate waters from the Norwegian Sea, nowadays termed Norwegian Sea Arctic Intermediate Water after Blindheim and Ådlansdsvik (1995), to form the outflow through the FBC. While after Read and Pollard (1992) relatively fresh water from the East Icelandic Current additionally contributes to overflowing water. The latter water mass is characterized by a salinity minimum and as it is modified by mixing with surrounding water it is termed Modified East Icelandic Water. Although the water mass names indicate origins in the Iceland and Norwegian Sea, only a part of the Norwegian Sea Intermediate Water is formed by sinking in the frontal region in the Norwegian Sea whereas the remaining part as well as the deep water flows from the Greenland Sea through the Jan Mayen Channel (Hansen and Østerhus, 2000).

The large-scale reorganization of the flow north of the Greenland Iceland Scotland Ridge, that leads to different water masses at the DS, is likely to affect also the pathways of the FBC overflow including possible changes in its water masses. Observational evidence exist for such changes on seasonal and on interannual to interdecadal timescales (Turrell et al., 1999; Borenäs et al. 2001; Eldevik et al., 2009). Similar to the previous section, water mass characteristics were computed to reveal the simulated changes over the period 1994-2003. A section upstream of the overflow (the Faroe-Shetland section along 52.4°N) was selected to minimized the effect of the substantial mixing in the FSC channel (e.g. Borenäs et al. 2001) that would not allow us to relate changing characteristics to changing pathways.

In the lighter fraction of the overflowing water shown in Fig. 7, a shift to more saline conditions can be observed from the years 1999 to 2003 which looks similar to the bimodal T-S characteristics which Borenäs et al. (2001) related to the absence or presence of IAIW water mass. However, the convexity due to the presence of fresh IAIW in the left (1999) curve is not very clearly pronounced in the simulation which shows a larger shift in the Norwegian Sea Intermediate Water instead. They also reported a seasonal dependence of the occurrence of the IAIW signal which the simulation partly confirms. Although, including the seasonal spread, water mass types for 1999 and 2003 will overlap, a clear difference between the states of 1999 in comparison to 2003, as the Fig. 7 illustrates, holds and the shift to more saline conditions from 1999 to 2003 is also in agreement with the observed variability in the FSC that Eldevik et al. (2009) recently reported. Although we find also reasonable agreement with the temperature and salinity changes in the North Atlantic Water, RAW, and the overflows as defined in their analysis (not shown), the shortness of period 1992–2004 does not allow us to follow along their line and analyse statistical relations with any significance. An attempt is therefore made to define two classes, FSC99 and FSC03, and an additional dense class, FSCdense, as indicated in Fig. 7 to allow for a later decomposition of the transports.

The sources of the FBC overflow can be divided into three paths: the East Icelandic Current, the shorter pathway through the Jan Mayen Channel and a deeper path of Norwegian Sea Arctic Intermediate Water from the Norwegian Sea. As for the DS, the change from high to low wind stress curl shifts the circulation patterns. Considering the layer thicknesses shown in Fig. 8, the pool of FSC99 water that is present in 1999 along the Arctic Front, is exported towards the FBC following a current along the Mohn and Jan Mayen Ridge system. A further fraction is exported northeastward into the Lofoten Basin. The pool moved southward and is much reduced in 2003 now additionally exporting water westward in a current north of Iceland, although due to mixing the signature is lost before it enters the entrance to the DS. From 1999 to 2003, a build up of FSC03 water is noticeable in the centre of the Lofoten Basin and a small fraction leaves this basin southward underneath the eastern branch of the Norwegian Atlantic Current. Käse et al. (2009) demonstrated the possibility of such a current in a circulation that is purely driven by a density difference across the Greenland Iceland Scotland Ridge or by a deep inflow through Fram Strait. The strong anticyclonic mesoscale feature visible in the centre of the Lofoten Basin is well observed and described in detail by Köhl (2007). It

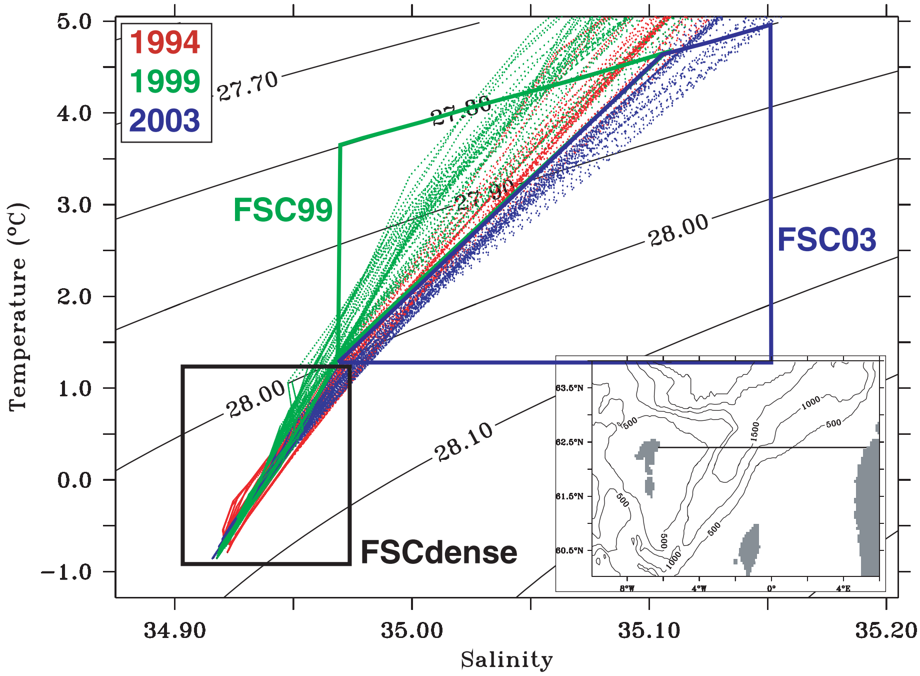

Fig. 7. T-S diagram of the water masses in the Faroe-Shetland Channel sampled along 62.5°N in the years 1994, 1999 and 2003.

is embedded into the cyclonic circulation of the Lofoten Basin (see also Fig. 2 of Käse et al., 2009.) According to Köhl (2007), it emerges from anticyclones which are shed by the Norwegian Atlantic Current and which are topographically guided into the centre of the Lofoten Basin where they merge. Both the cyclonic circulation of the basin and the anticyclonic circulation of the vortex are indicated by the float trajectories shown in Søiland et al. (2008). However, the vortex remains rather inactive for the distribution of the overflowing water masses.

The low-salinity part of the FSCdense includes a large fraction of the previously defined DKdense water mass. It is therefore inevitable that both classes reveal common features. Particularly, the thickening in the Greenland Sea from 1999 to 2003 and the reduction of the EGC is a dominant feature of both patterns. However, the circulation of FSCdense additionally reveals more details in the Iceland and the Norwegian Sea. A large fraction of the FSCdense water in the Greenland Sea is not part of DKdense and will therefore not exit through the DS. Particularly near the Jan Mayen Fracture Zone, a large volume of FSCdense exists that flows eastward into the Norwegian Sea in 1999 and which largely has disappeared in 2003. The transports north of Iceland reverse from eastward to westward and the strong southward current following the Jan Mayen Ridge weakened in 2003. The water flowing along these pathways seems not to follow directly into the entrance of FBC but a large part flows northward roughly along 2°W and is buffered in the Norwegian Sea. Consequently, a larger volume has build up there in 1999. In 2003, the direction of the flow along 2°W is reversed and similar to what was seen above in the layer of the FSC03 class, water from the Norwegian Sea follows the eastern path along the Norwegian shelf edge feeding the FBC overflow (note, east of this current the flow is always southward). In the idealized experiments by Käse et al. (2009), the reversal of this current can be induced by a switch from deep to shallow inflow through Fram Strait. Hansen et al. (2001) related the FBC overflow to the depth of isopycnals at the Ocean Weather Ship Mike which, however, was no longer supported by more recent measurements of Hansen and Østerhus (2007) who consequently uttered doubts about the weakening of the FBC-overflow in the 1950–2000 period that Hansen et al. (2001) reported. The eastern path may communicate changes at Mike into the FSC and may thus enable a relation between interface changes and the FSC overflow. However, the path of communication is altered by the strength of the wind stress curl.

Considering the contributions of the three water mass classes to the FBC overflow transport variability, the decomposition of the transport shown in Fig. 9b demonstrates that FSC99 and FSC03 have only a minor contribution to the transports with very small changes after 1999. The time variability is thus explained entirely by the dense fraction that carries almost the total transport. However, the upstream volume changes of the three classes (Fig. 9a) are equally large, with nearly perfectly anticorrelated variability between the FSC99 and FSC03 volumes ($r = 0.95$). Because the export of FSC99 and FSC03 is small and nearly constant, formation and transformation are the major factors to explain the covariability. The relatively fresh FSC99 water that is formed near the frontal region is exported into the Lofoten basin

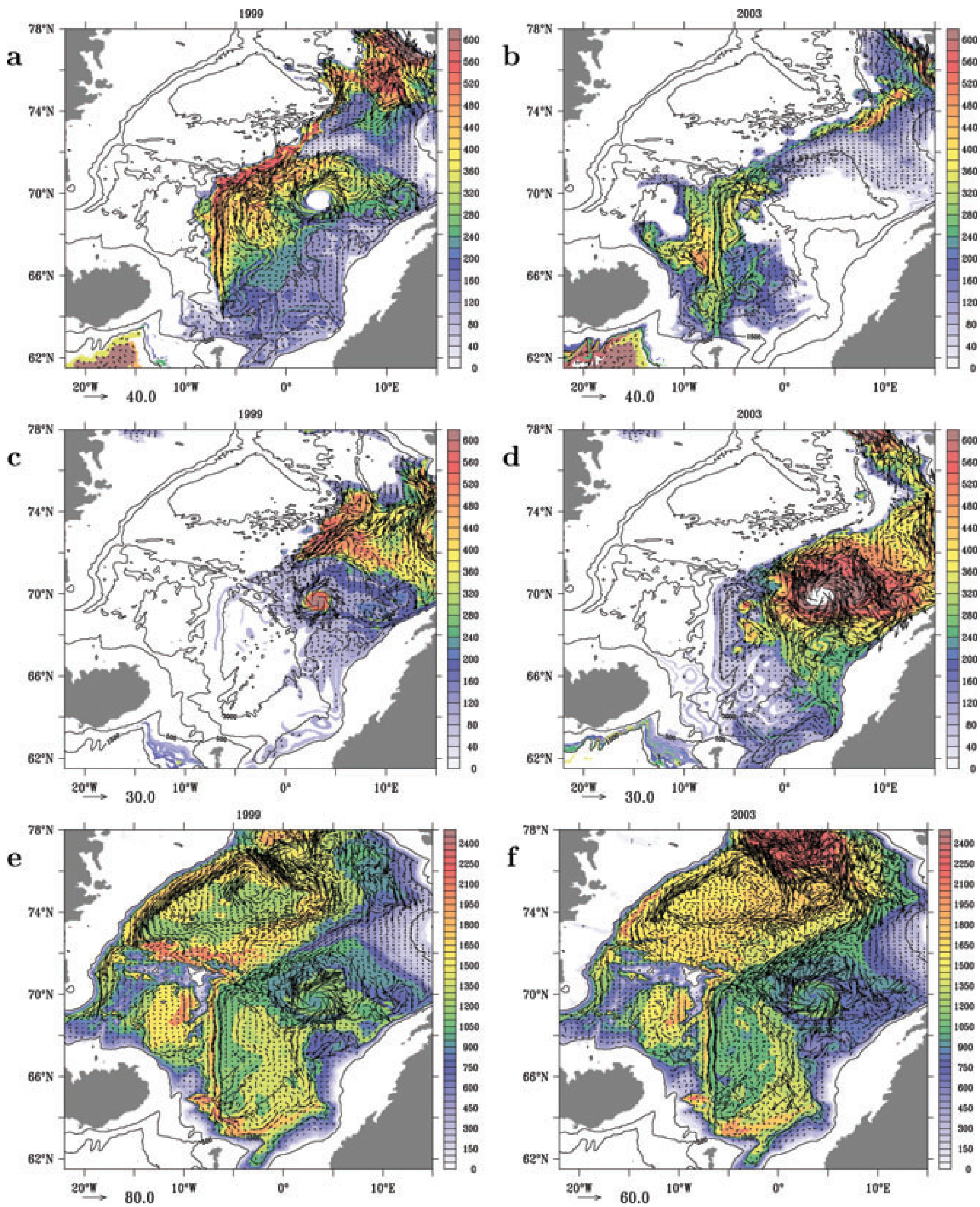

Fig. 8. Layer thickness (in m) of different water mass classes. Shown are years of high and low wind stress curl (1999, 2003) for the classes FSC99 (a,b), FSC03 (c,d) and FSCdense (e,f). Transport densities (in $m^2\ s^{-1}$) from vertically integrating velocities in the respective layers are overlaid.

(Fig. 8a) where it partly becomes entrained into the overlying saline water by winter time convection. This process explains the newly formed water of the FSC03 volume that is visible in the centre of the Lofoten Basin in 2003. After 1994, there seems to be a reasonably good correlation between the FSCdense volume and the FSC overflow although most of the additional volume is located just south of Fram Strait and in the Greenland Sea and seems to be fairly isolated from the FSC. According to Käse et al. (2009), the deep inflow through Fram Strait establishes a regime similar to a flow purely driven by a density difference across the Greenland Iceland Scotland Ridge, that leads to larger FSC transports, as opposed to shallower inflow through the Fram Strait that promotes DS overflow.

At last, we want to trace the pathways of the FBC overflow water by backward floats for the two different regimes. For 1999, a large fraction of the water is originating from the southward

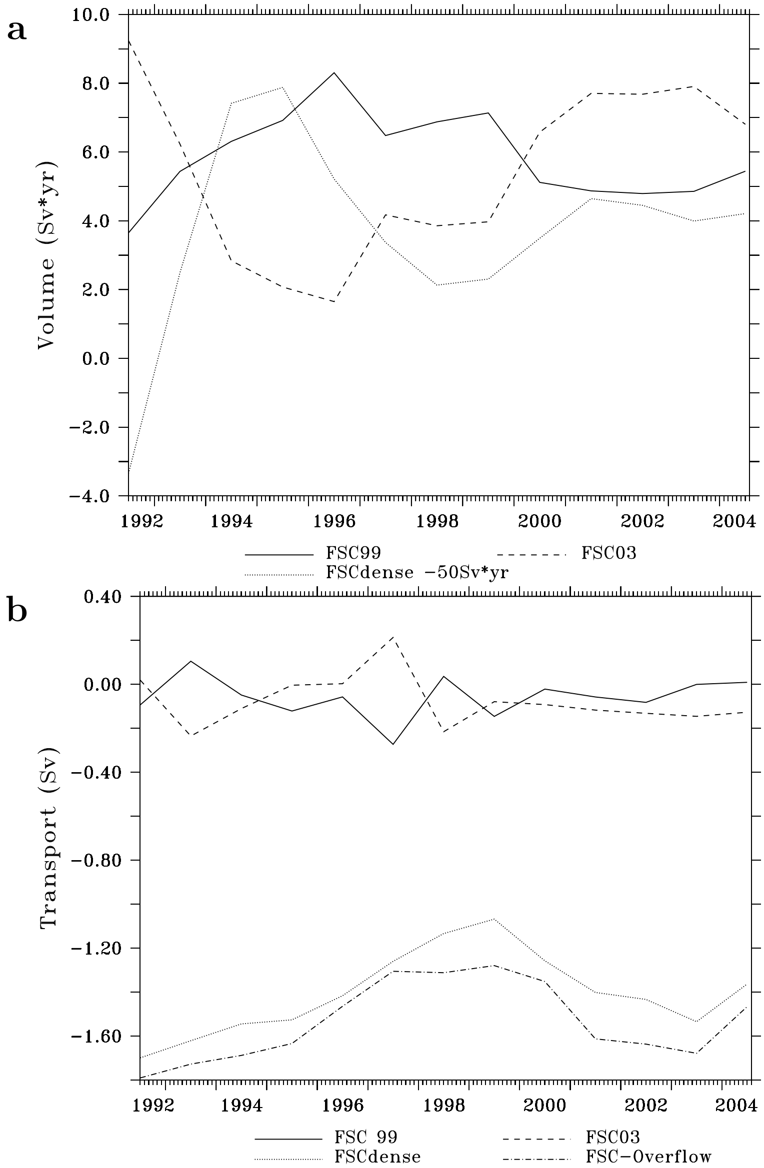

Fig. 9. Total volume of the water in the density classes FSC99, FSC03 and FSCdense (a) and their contributions to the FSC overflow calculated as transports across 62.4°N east of Faroe Islands below $\sigma_\Theta = 27.8$.

flow along the Norwegian shelf edge (Fig. 10a) while a smaller fraction follows along the faster pathway along the Jan Mayen Ridge. For longer time scales, the floats originate also from the eastern basins and the EGC by crossing over north of Iceland and along the Jan Mayen Fracture Zone. In 2003, the eastern branch is the only supply for water while only for longer time scales (2002 and 2001) the two western pathways, mostly along the Jan Mayen Ridge, become active.

5. Sensitivity of the overflows to interface height changes

Adjoint sensitivities calculations are a tool to determine regions and mechanisms that contribute to changes of a target quantity. One of the first ocean applications of these sensitivities was the calculation of regions that influence the heat transport in the North Atlantic (Marotzke et al., 1999). In this process, an adjoint model is used to efficiently calculate gradients (or sensitivities) of a quantity with respect to perturbations of certain parameters of the model.

Here we calculate December 1999 and 2003 sensitivities of the monthly mean overflow through DS and FBC. The calculations are done with the low-resolution version of the model which shows slightly lower mean transports through DS and FBC with basically the same temporal variability. The discussion will focus on sensitivities to interface height changes. Although many causes of changes for the DS and FSC overflow exist (e.g. Biastoch et al., 2003; Lake and Lundberg, 2006; Köhl et al., 2007b; Käse et al., 2009), there is a general agreement that the overflows on both sides of Iceland are hydraulically controlled

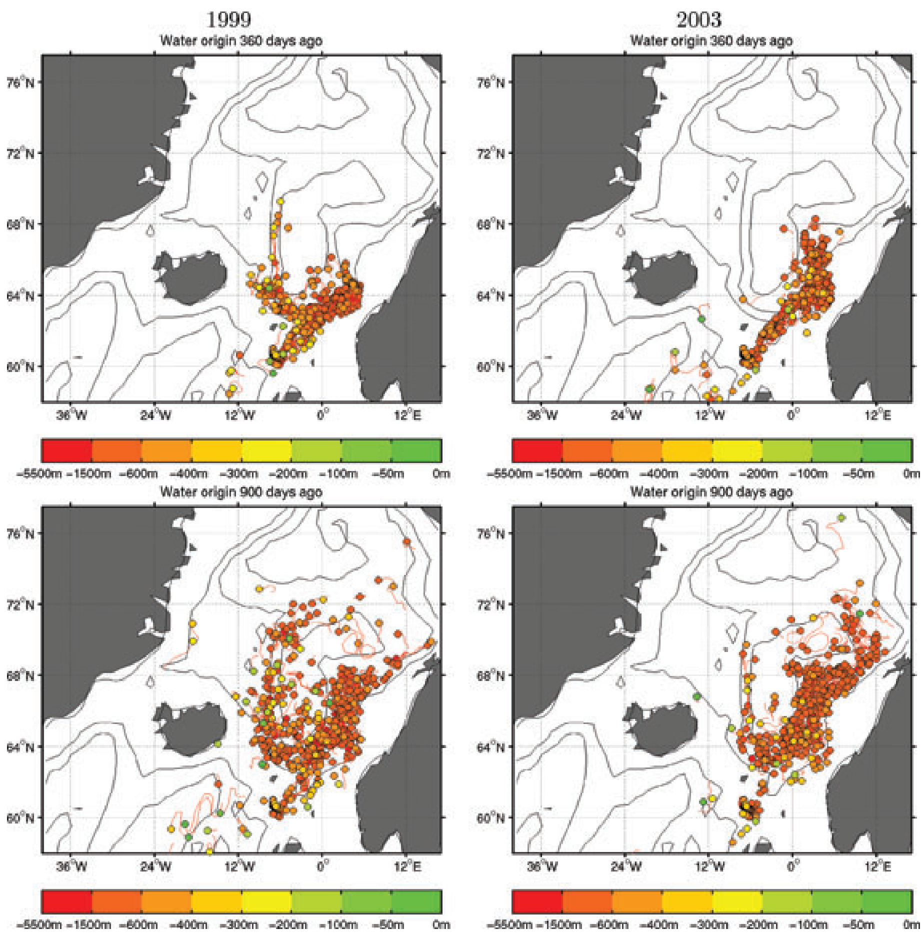

Fig. 10. Backward float positions with path of the last 30 days and its depth indicated by colour. 1000 floats were seeded along 7°W roughly below $\sigma_\Theta = 27.8$ in year 1999 (left panels) and 2003 (right panels), respectively and integrated backward for periods as indicated in the panels.

(e.g. Käse et al., 2003; Girton et al., 2006). In hydraulic control theory, changes of the flow through a strait depend within the approximation of a two-layer fluid only on the height of the interface upstream.

For the DS overflow, in the simple relation

$$\Delta \mathrm{DSO} = \frac{\partial \mathrm{DSO}}{\partial h_{27.8}} \Delta h_{27.8}, \quad (1)$$

the sensitivities $\partial\mathrm{DSO}/\partial h_{27.8}$ describe at which locations perturbations of the local height of the $\sigma_\Theta = 27.8$ surface ($\Delta h_{27.8}$) will change the DS overflow most.

Hansen et al. (2001) proposed a relation between the remote reservoir height as measured by Ocean Weather Ship Mike and the FBC overflow. This relation was questioned by Helfrich and Pratt (2003) and Pratt (2004) because the predicted transport is very far from the actual location. They argued that, if the location of the source changes, the flow through the strait may stay constant even though the reservoir height changes at a certain location. Two questions emerge: first, where is this upstream reservoir located, especially, how large is the area and how does this change if lags are considered, secondly, how do the different forcing mechanisms ultimately change the reservoir height. Although the second question is more important, it is much harder to address and we will therefore restrict the discussion to the first question which can be addressed by the sensitivities of the transports to reservoir height changes as shown in Fig. 11.

Figure 11a shows the sensitivity of the December 1999 DS overflow to $h_{27.8}$ changes in the same month which therefore describes the reservoir of an immediate response. Positive sensitivities indicate regions where increasing the reservoir height enhances the transport. Accordingly, the main upstream reservoir for the DS overflow lies very localized directly upstream on the right hand side (looking downstream of the flow) of the channel. Negative sensitivities are located to the left enhancing the southward deep layer transport according to the geostrophic relation. Additional negative sensitivities are located along the eastern shelf of Iceland, along the northern part of the Iceland-Faroe Ridge and at the entrance of the FSC. Switching to the

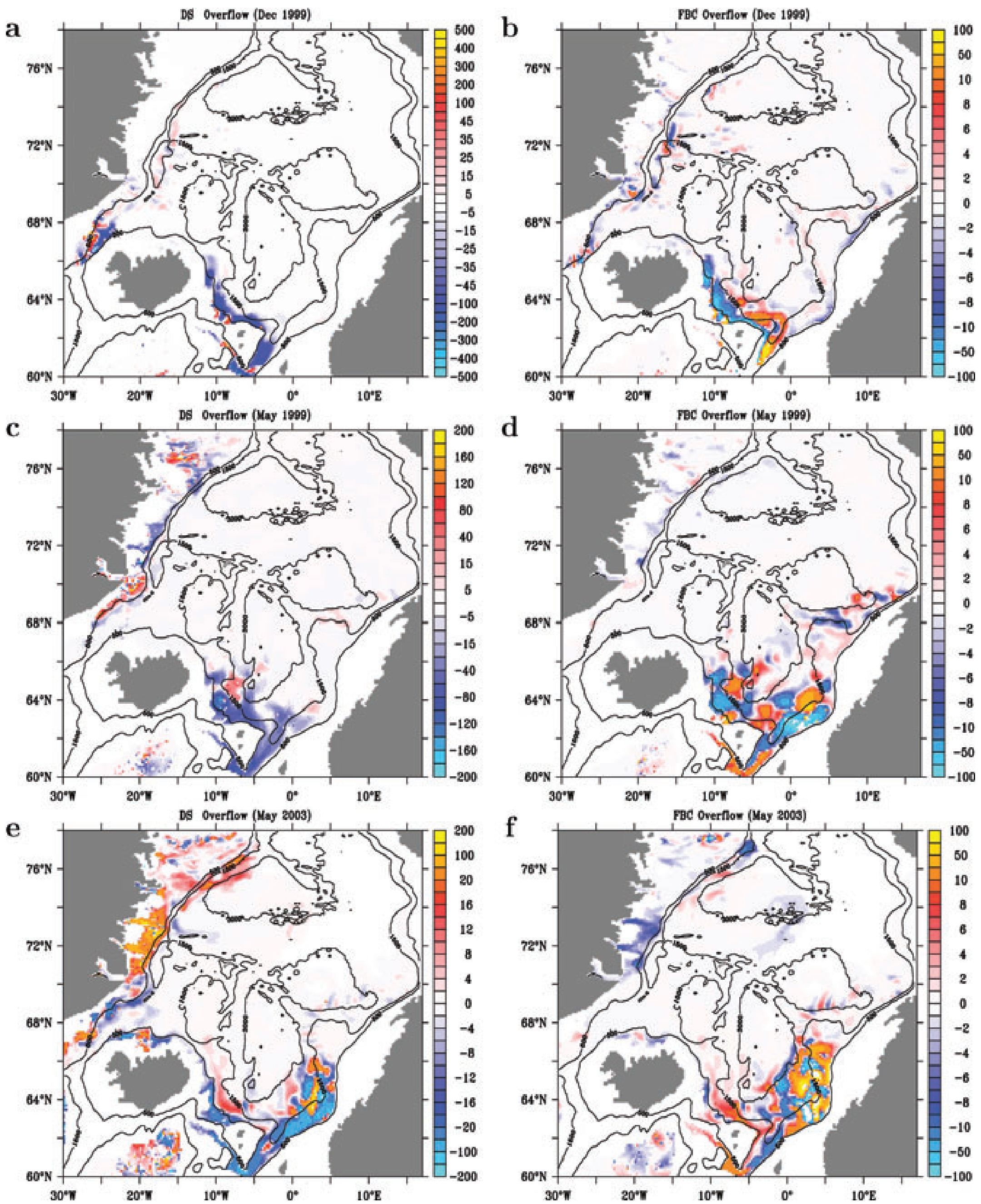

Fig. 11. Sensitivity of the Denmark Strait (a,c,e) and Faroe-Shetland (b,d,f) overflow of December 1999 to interface height changes in December 1999 (a,b) and 6 months before in May 1999 (c,d). Panel (e) and (f) show the Sensitivity of the December 2003 overflows to interface height changes 6 months before. The interface is the height of the $\sigma_\Theta = 27.8$ surface. Values are in m^3 km$^{-1}s^{-1}$.

FBC overflow (Fig. 11b), reveals similar patterns with regionally reversed signs. The upstream reservoir for the FBC overflow lies directly in the FBC and extends westward along the Jan Mayen Ridge. In comparison to the DS sensitivity, the pattern along the Norwegian shelf slope and into the DS have a reversed sign.

A reversal of sign is expected because a larger transport in one of the overflows has to be compensated by either a larger upper layer inflow or a reduced overflow on the other side of Iceland because the net northward transport is prescribed to be 1 Sv. Because the former will not be very sensitive to interface changes, in most areas the sign reverses promoting either cyclonic or anticyclonic circulation anomalies around Iceland. Only along the eastern Icelandic shelf and north of the Iceland-Faroe Ridge sensitivities are negative for both cases. The reservoir area obviously belongs to the so far neglected Iceland-Faroe Ridge overflow which affects the DS and FSC overflow in the same way. The result is surprising because the mean overflow transport across Iceland-Faroe Ridge is only 0.02 Sv (Köhl et al., 2007b). However, the temporal variability of this overflow is quite large with instantaneous transport values exceeding 2 Sv.

On longer time scales, propagation of density anomalies become more important. We show sensitivities to $h_{27.8}$ changes 6 months before for both overflows for the high and low wind stress curl cases. For the large wind stress curl case (Figs 11c and d), DS sensitivities propagate mainly along the EGC concentrating in agreement with the backward floats shown in Fig. 6 at 70°N. For the FSC sensitivity, the two pathways east of Iceland are present as two isolated areas of positive sensitivities roughly at 3°E, 63°N and 2°W, 64°N. An additional area is visible at 7°W, 65°N that also exists in Fig. 11c and that originates in both cases from the Iceland-Faroe Ridge. The situation changes during a low wind stress curl (Fig. 11f). Here, the western branch along the Jan Mayen Ridge is much reduced in comparison to the high wind stress curl case. The eastern branch dominates and positive sensitivity reaches the position of Weather Ship Mike at 0°, 66°N in May, 6 months prior to the overflow response which supports the 8-month-delayed linkage between the magnitude of the overflow and the upstream reservoir conditions suggested by Hansen et al. (2001). A comparison with Fig. 11d reveals that the propagation speed of the sensitivities may depend on the forcing conditions, which may lead to a loss of coherence of the two signals for a fixed lag during certain periods also noted by Hansen and Østerhus (2007). The two panels also illustrate the argument of Pratt (2004) that as the upstream flow path may change the location of the reservoir will also move. As shown in Figs 11a and b, the problem is resolved if one moves closer to the entrance of the sill; the controlling region for the instantaneous overflow is then relatively small and always located near the sill. The interesting new result different from steady solutions regarded by Helfrich and Pratt (2003) is the dynamical aspect of the reservoir height. The reservoir height is advected with the flow and will causes a response of the overflow with a certain time lag. The origin of overflow anomalies can therefore be traced back to upstream changes.

At last, DS sensitivities are regarded again. Although from the results of Section 3, the EGC branch is expected to be much reduced during low wind stress curl situations (Fig. 11e), a large sensitivity pattern is visible along the EGC branch whereas no sensitivity patterns are visible in the Iceland Sea. However, the propagation of sensitivities reveal no apparent link to the DS and the pattern seems to emerge from a local instability. In summary, for the FBC overflow the advection of interface height anomalies seems to be a relevant mechanism whereas for the DS indications for such a mechanism exist only during high wind stress curl forcing.

6. Conclusions

By analysing numerical ocean model results, we investigate changing water masses and source regions of the overflows west and east of Iceland under high and low wind stress curl forcing conditions. As previously noted, changes in water mass characteristics indicate changes of source regions and vice versa. Although a close correspondence between modelled and observed water masses could not be established, a validation with simulated backward float trajectories show that the characteristics are still a valid means to reveal changing pathways. From this analysis, a slightly modified circulation scheme emerges that is presented in Fig. 1. From analysing a series of sections from the Fram Strait to the DS, Rudels et al. (2002) concluded that the main source of the DS overflow is the EGC with contributions from the Iceland Sea, contradicting the early notion of Swift et al. (1980) who described the upper Arctic Intermediate Water formed in the Iceland Sea as the main source. In agreement with Rudels et al. (2002), our circulation scheme suggests during moderately strong wind stress curl in 1999 the main source of the DS overflow to be the EGC, whereas in the model during periods with low wind stress curl the source is in the Iceland Sea and signatures of warmer and saltier water are found in the lighter fraction of the overflow. In contrast, for the very high NAO year 1990 Rudels et al. (2002) reports a larger contribution from the Iceland Sea due to mixing which then results into colder and fresher DS overflow water characteristics. Three cases emerge from this: first, during moderate wind stress, water is brought by the EGC to the DS while the Iceland Sea is a receiver and the cyclonic circulation in the Iceland Sea entrains Atlantic Water from the Irminger Current and the Arctic Front. Secondly, during low forcing conditions, the cyclonic circulation in the Iceland Sea relaxes and the basin is able to directly export water leading to a predominant source from the Iceland Sea which releases high salinity near surface water that was entrained during moderate forcing conditions. Thirdly, during very high wind stress a strong EGC leads to an enhanced mixing of the EGC water with the water from the Iceland Sea which thus indirectly contributes to the overflow water and leads the coldest temperature characteristics.

As the forcing goes from high to low wind stress curl, the westward current north of Iceland, which according to Jonsson (1999) identifies the Iceland Sea as the main contributor to the DS overflow, is found to change its direction. At the same time, the contribution to FBC overflow from a path along the slopes north of the Faroes intensifies. The existence of these currents and the related changes can be rationalized considering the potential vorticity budget of the dense layer circulation in the Nordic Seas. Helfrich and Pratt (2003) consider the budget in a basin with inflow on one side and outflow on the other side with an optional interior downwelling source. Without this source, the conservation of potential vorticity leads to a split into two boundary currents and a symmetric flow along f/H contours, for example the eastern and the western boundary of the basin. When the source is represented by interior downwelling, the outflow implies an anticyclonic circulation along the eastern boundary. In the Nordic Seas, inflow is represented by the flow through the Fram Strait and outflow by the overflows. However, the picture is complicated by a separation of the basin in four subbasins and two outflows. Simplifying the circulation by regarding only two basins (the eastern basins of the Norwegian Sea and the western basins of the Iceland and Greenland Sea), the linearity of the balance implies that the total circulation is a superposition of the circulations in the individual basins.

The case of an interior source is also realized in the DAM BREAK experiment of Käse et al. (2009) shown in their Fig. 5a. Although there is no interior source, because it is a non-stationary case the condition of only outflow implies anticyclonic circulation in both subbasins represented be a strong southward flow along the Mohn Ridge and along the Norwegian shelf. Including inflow of dense water from the north, the flow is closer to stationarity and more symmetric in both basins with a strong East Greenland Current and southwestward flow along the slope north of the Faroes (see their Fig. 5b). As it is part of the anticyclonic branch, in both cases the flow north of Iceland is westward. In our model about 1.7 Sv dense (below $\sigma_\Theta = 27.8$) water enters through Fram Strait while about 4.1 Sv leaves through the overflows. This implies a net outflow balanced by an interior source which in turn implies an anticyclonic circulation of the dense water. Superimposed on this purely density driven circulation is the wind driven barotropic circulation which is cyclonic. The composition is visible in Fig. 2 of Käse et al. (2009), showing a cyclonic circulation in the interior of the basins with smaller anticyclonic parts further up the slopes north of Iceland and along the Norwegian Shelf. The anticyclonic part of the circulation is enhanced during conditions with weak cyclonic wind stress and vice versa implying that during strong forcing the current north of Iceland reverses to a westward flow and the current along the Norwegian shelf intensifies as it is seen for the switch from 1999 to 2003.

In a tracer release experiment (Eldevik et al., 2005), investigated the spreading of the Greenland Sea water through the Nordic Seas to the overflows in high and low NAO conditions that correspond to high low wind stress curl conditions and provided a circulation scheme very similar to Fig. 1. During high NAO, the barotropic circulation is enhanced in the Nordic Seas (Furevik and Nilsen, 2005) and in agreement with Eldevik et al. (2005), our simulation confirms their finding that the intensified circulation is related to larger currents connecting the Greenland and the Norwegian Sea along Jan Mayen Fracture Zone leading to a more direct connection of the Greenland Sea Water to the FSC. During low NAO, they found that the Jan Mayen Current and the shortcut have disappeared and the meridional flow in the Norwegian Basin is less pronounced. However, in contrast to Eldevik et al. (2005), who claim that during low NAO the pathway taken by the Greenland Sea Water exported at DS is the EGC, we find a general absence of this path during low wind stress curl. Moreover, their slower path of water that does not leave at the DS and consequently travels through the Iceland and Norwegian Sea to the FBC during low NAO, although present in the scheme in Fig. 1, is mainly a feature of high wind stress curl conditions in our model. Differences may arise since after the mid-1990s the wind stress curl around Iceland and the NAO are less tightly related to the NAO as the NAO centre of action shifts northeastward (Zhang et al., 2008). Following these changes, the sources of the FBC overflows change from a two path system during high wind stress curl conditions with additional contributions from the East Icelandic Current to mainly a single source with water spreading only along the Norwegian Shelf slope in contrast to Søiland et al. (2008) who sees the current along the slope north of the Faroe as the exclusive source of the FBC overflow. However, changes in water masses and pathways are found to be consistent with the findings of Borenäs et al. (2001) and can be rationalized by the idealized case of Helfrich and Pratt (2003). Similar to the explanation for the current north of Iceland earlier, the southward flow along the Norwegian continental slope is also part of the anticyclonic circulation that is enhanced during low wind stress forcing, whereas the flow north of the Faroe, which is part of the cyclonic basin circulation is stronger during high wind forcing.

Recently, Eldevik et al. (2009) presented a different analysis of temperature and salinity changes at the DS and FBC based on statistical relations. They explain changes in the overflow over the period 1950–2005 by advection of anomalies that originate from the Atlantic inflow, whereas the current manuscript associates water mass changes with changes in origin due to different circulation regimes. Both interpretations are simplified views, one is approximating the circulation in the Nordic Seas as unchanged whereas the other does the same for the background water masses. In reality, both processes are likely to play a role and the interplay between both should be considered. However, wind driven circulation changes provide a fast means to change the water masses intermittently while advection should play a role on longer time scales. To this end, Eldevik et al. (2009) describe only changes on time scales longer than 5 years. A timescale argument might thus provide a means to separate these complementary mechanisms that seem to provide contradictory explanations at first. Both analyses leave also room for unaccounted processes.

Modelling the spreading and mixing of water masses are up to now the most difficult tasks for ocean models. Therefore, the level of agreement between the model results and observed data remains rather qualitative and is based on relative simple means of comparison. However, the analysis of changes of water masses and their associated pathways in the Nordic Seas revealed numerous findings that observations could confirm. Some inconsistencies remain, particularly, the separation between the circulation states for high and low wind stress curl states may not be as clear in the real world and certainly also not as easy to see in the observations. The situation is additionally complicated as the relation of wind stress curl around Iceland to the NAO is changing since the mid 1990s.

7. Acknowledgments

Nuno Serra provided valuable comments on the paper and the backward float program was developed by Robert Landsberger. This work was supported by Sonderforschungsbereich 512 of the Deutsche Forschungsgemeinschaft and is a contribution to CliSAP. The integration of the model was performed at the German high-performance computing centre DKRZ.

References

Aagaard, K., Swift, J.H. and Carmack, E.C. 1985. Thermohaline circulation in the Arctic Mediterranean Seas. *J. Geophys. Res.***90**, 4833–4846.

Biastoch, A., Käse, R. and Stammer, D. 2003. The sensitivity of the Greenland-Scotland Ridge overflow to forcing changes. *J. Phys. Oceanogr.* **33**, 2307–2319.

Blindheim, J. and Ådlansdsvik, B. 1995. Episodic formation of intermediate water along the Greenland Sea Arctic Front. *ICES CM 1995/Mini:6*, 11 pp.

Borenäs, K.M., Lake, I.L. and Lundberg, P.A. 2001. On the intermediate water masses of the Faroe-Bank Channel overflow. *J. Phys. Oceanogr.* **31**, 1904–1914.

Bryden, H.L., Longworth, H.R. and Cunningham, S.A. 2005. Slowing of the Atlantic meridional overturning circulation at 25°N. *Nature* **436**, 655–657.

Dickson, R., Lazier, J., Meincke, J., Rhines, P. and Swift, J. 1996. Longterm coordinated changes in the convective activity of the North Atlantic. *Prog. Oceanogr.* **38**, 241–295.

Dickson, B., Yashayaev, I., Meincke, J. and Turrell, B. 2002. Rapid freshening of the deep North Atlantic Ocean over the past four decades. *Nature* **416**, 832–836.

Dickson, B., Dye, S., Jónsson, S., Köhl, A., Macrander, A. and co-authors. 2008, Arctic-Subarctic Ocean Fluxes: Defining the role of the Northern Seas in Climate, Springer, Dordrecht, The Netherlands, pp. 443–474.

Dickson, R.R. and Brown, J. 1994. The production of North Atlantic deep water: sources, rates, and pathways. *J. Geophys. Res.* **99**, 12319–12341.

Eldevik, T., Straneo, F., Sando, A.B. and Furevik, T. 2005. Pathways and export of Greenland Sea water. *The Nordic Seas: An integrated perspective* (eds. H. Drange, T. M. Dokken, T. Furevik, R. Gerdes and W. Berger), Geophysikal Monography Series, AGU, 89–105.

Eldevik, T., Nilsen, J.E.Ø., Iovino, D., Olsson, K.A., Sandø, A.B. and co-authors. 2009. Observed sources and variability of Nordic Seas overflow. *Nat. Geosci.* **2**, 406–410.

Gaillard, F. G.,Autret, E., Thierry, V., Galaup, P., Coatanoan, C. and co-authors. 2009. Quality control of large argo data sets. *J. Atmos. Ocean. Tech.* **26**, 337–351.

Furevik, T. and Nilsen, J.E. Ø. 2005. Large-scale atmospheric variability and its impact on the Nordic Seas ocean climate—a review in. *The Nordic Seas: An integrated perspective* (eds. H. Drange, T. M. Dokken. T. Furevik. R. Gerdes and W. Berger), Geophysikal Monography Series, AGU, 105–136.

Giering, R. and Kaminski, T. 1998. Recipes for adjoint code construction. *ACM Trans. Math. Software* **24**(4), 437–474.

Girton, J.B., Sanford, T.B. and Käse, R.H. 2001. Synoptic sections of the Denmark Strait overflow. *Geophys. Res. Lett.* **28**, 1619–1622.

Girton, J.B., Pratt, L.J., Sutherland, D.A. and Price, J.F. 2006. Is the faroe bank channel overflow hydraulically controlled? *J. Phys. Oceanogr.* **36**, 2340–2349.

Häkkinen, S. 2007. Upper ocean T-S variations in the Greenland Sea and their association to climatic conditions. *J. Geophys. Res.* **112**, doi:10.1029/2006JC003498.

Hansen, B. and Østerhus, S. 2000. North Atlantic–Nordic Seas exchanges. *Prog. Oceanogr.* **45**, 109–208.

Hansen, B. and Østerhus, S. 2007. Faroe Bank overflow 1995–2005. *Prog. Oceanogr.* **52**, 817–856.

Hansen, B., Turrell, W.R. and Østerhus, S. 2001. Decreasing overflows from the Nordic Seas into the North Atlantic Ocean through the Faroe Bank Channel Science 1950. *Nature* **411**, 927–930.

Helfrich, K.R. and Pratt, L.J. 2003. Rotating hydraulics and upstream basin circulation. *J. Physical. Oceanogr.* **33**, 1651–1663.

Hoteit, I., Cornuelle, B., Köhl, A. and Stammer, D. 2005. Treating strong adjoint sensitivities in tropical eddy-permitting variational data assimilation. *Q. J. Met. Soc.* **613**, 3659–3682.

Jeansson, E., Jutterström, S., Rudels, B., Rudels, B., Anderson, L.G. and co-authors. 2008. Sources to the East Greenland Current and its contribution to the Denmark Strait overflow. *Prog. Oceanogr.* **78**, 12–28.

Jonsson, S. 1999. The circulation in the northern part of the Denmark Strait and its variability. *ICES CM,* 9.

Jónsson, S. and Valdimarsson, H. 2004. A new path for the Denmark Strait overflow water from the Iceland Sea to Denmark Strait. *Geophys. Res. Lett.* **31**, L03305.

Käse, R.H., Girton, J.B. and Sanford, T.B. 2003. Structure and variability of the Denmark Strait overflow: model and observations. *J. Geophys. Res.* **108**, doi:10.1029/2002JC001548.

Käse, R.H., Serra, N., Köhl, A. and Stammer, D. 2009. Mechanisms for the variability of dense water pathways in the Nordic Seas. *J. Geophys. Res.* **114**, C01013, doi:10.1029/2008JC004916.

Köhl, A. 2007. Generation and stability of a quasi-permanent vortex in the Lofoten Basin. *J. Phys. Oceanogr.* **37**, 2637–2651.

Köhl, A., Stammer, D. and Cornuelle, B. 2007a. Interannual to decadal changes in the ECCO global WOCE synthesis. *J. Phys. Oceanogr.* **37**, 313–337.

Köhl, A., Käse, R.H., Stammer, D. and Serra, N. 2007b. Causes of changes in the Denmark Strait Overflow. *J. Phys. Oceanogr.* **37**, 1678–1696.

Lake, I. and Lundberg, P. 2006. Seasonal barotropic modulation of the deep-water overflow through the Faroe Bank Channel. *J. Phys. Oceanogr.* **36**, 2328–2339.

Large, W.G. and Yaeger, S.G. 2004. Diurnal to decadal global forcing for ocean and sea-ice models: the data sets and flux climatologies. *NCAR Technical Note* 105.

Large, W.G., Williams, J.C. and Doney, S.C. 1994. Ocean vertical mixing: a review and a model with a nonlocal boundary layer parametrization. *Rev. Geophys.* **32**, 363–403.

Levitus, S. and Boyer, T. P. 1994. Temperatures. Vol. 4, World Ocean Atlas 1994. *NOAA Atlas NESDIS*, 117.

Levitus, S., Burgett, R. and Boyer, T.P. 1994. Salinity. Vol. 3, World Ocean Atlas 1994. *NOAA Atlas NESDIS*, 99.

Macrander, A., Send, U., Valdimarsson, H., Jónsson, S. and Käse, R.H. 2005. Interannual changes in the overflow from the Nordic Seas into the Atlantic Ocean through Denmark Strait. *Geophys. Res. Lett.* **32**, L06606.

Marotzke, J., Giering, J.R., Zhang, Q.K., Stammer, D., Hill, C.N. and co-authors. 1999. Construction of the adjoint MIT ocean general circulation model and application to Atlantic heat transport sensitivity. *J. Geophys. Res.* **104**, 29 529–29 548.

Mauritzen, C. 1996. Production of dense overflow waters feeding the North Atlantic across the Greenland-Scotland Ridge. 1. Evidence for a revised circulation scheme. *Deep Sea Res. I* **43**, 769–806.

Olsson, K.A., Jeansson, E., Tanhua, T. and Gascard, J.-C. 2005. The East Greenland Current studied with CFCs and released sulphur hexafluoride. *J. Mar. Syst.* **55**, 77–95.

Olsen, S.M., Hansen, B., Quadfasel, D. and Østerhus, S. 2008. Observed and modelled stability of overflow across the Greenland-Scotland Ridge. *Nature* **455**, 519–523, doi:10.1038/nature07302.

Poulain, P.-M.,Warn-Varnas, A. and Niiler, P.P. 1996. Near surface circulation of the Nordic Seas as measured by Lagrangian drifters. *J. Geophys. Res.* **101**, 18 237–18 258.

Pratt, L.J. 2004. Recent progress on understanding the effects of rotation in models of sea straits. *Deep Sea Res. II* **51**, 351–369.

Quadfasel, D. and Käse, R. 2007. Present-day manifestation of the Nordic Seas overflows. *Ocean Circulation: Mechanisms and Impacts, Geophys. Monograph Series* **173**, 75–89.

Read, J.F. and Pollard, T. 1992. Water masses in the region of the Iceland-Faroes front. *J. Phys. Oceanogr.* **22**, 1365–1378.

Rudels, B., Fahrbach, E., Meincke, J., Budeus, G. and Eriksson, P. 2002. The East Greenland Current and its contribution to the Denmark strait overflow. *ICES J. Mar. Sci.* **59**, 1133–1154.

Rudels, B., Eriksson, P., Buch, E., Budéus, G., Fahrbach, E. and co-authors. 2003. Temporal switching between sources of the Denmark Strait overflow water. *ICES Marine Sci. Symp.* **219**, 319–325.

Schmitz, W.J. and McCartney, W.S. 1993. On the North Atlantic circulation. *Rev. Geophys.* **31**(1), 29–49.

Serra, N., Käse, R.H., Köhl, A., Stammer, D. and Quadfasel, D. 2010. On the low-frequency phase relation between the Denmark Strait and the Faroe-Bank Cannel overflows. *Tellus* **62A**, this issue.

Smethie, W.M. and Swift, J.H. 1989. The tritium:krypton-85-age of Denmark Strait overflow water and the Gibbs Fracture Zone water just south of Denmark Strait. *J. Geophys. Res.* **94**, 8265–8275.

SØiland, H., Prater, M.D. and Rossby, T. 2008. Rigid topographic control of currents in the Nordic Seas. *Geophys. Res. Lett.* **35**, doi:10.1029/2008GL034846.

Swift, J.H. and Aagaard, K. 1981. Seasonal transitions and water mass formations in the Iceland and Greenland seas. *Deep Sea Res.* **28**, 1107–1129.

Swift, J.H., Aagaard, K. and Malmberg, S. 1980. The contribution of Denmark Strait overflow to the deep North Atlantic. *Deep Sea Res.* **27**, 29–42.

Tanhua, T., Olsson, K.A. and Jeansson, E. 2005. Formation of Denmark Strait overflow water and its hydro-chemical composition. *J. Marine Syst.* **57**, 264–288.

Turrell, W.R., Slesser, G., Adams, R.D., Payne, R. and Gillibrand, P.A. 1999. Decadal variability in the composition of Faroe Shetland Channel bottom water. *Deep Sea Res. I* **46**, 1–25.

Willebrand, J., Barnier, B., Böning, C., Dieterich, C., Killworth, P.D. and co-authors. 2001. Circulation characteristics in three eddy-permitting models of the North Atlantic. *Prog. Oceanogr.* **48**, 123–161.

Zhang, J.L. and Rothrock, D. 2000. Modeling Arctic sea ice with an efficient plastic solution. *J. Geophys. Res.* **105**, 3325–3338.

Zhang, X., Sorteberg, A., Zhang, J., Gerdes, R. and Comiso, J.C. 2008. Recent radical shifts of atmospheric circulations and rapid changes in arctic climate system. *Geophys. Res. Lett.* **35**, doi:10.1029/2008GL035607.